PHYSICAL REVIEW B VOLUME 44, NUMBER 7 15 AUGUST 1991-I

Coverage and temperature dependence of the morphology of strained metal overlayers: Deposition of Pd on a bcc(110) substrate

Barry C. Bolding and Emily A. Carter
Department of Chemistry and Biochemistry, University of California, Los Angeles, California 90024-1569
(Received 26 February 1991)

The structure of Pd thin films deposited on a bcc(110) substrate has been investigated for coverages ranging from 0.25 to 3.50 bcc equivalent monolayers (ML) and temperatures from 75 to 500 K using molecular-dynamics and Monte Carlo simulation techniques. A pseudomorphic Pd bcc thin film is found to be metastable at low temperatures for all coverages studied. At high temperature, the Pd thin film is only pseudomorphic for coverages below 1.0 ML and rapidly undergoes a phase transition to an incommensurate fcc film above 1.0 ML. Low-energy electron-diffraction (LEED) patterns are calculated from the simulated configurations and compared to experimental results to demonstrate that two-dimensional wavelike structures in the Pd adlayer may be responsible for observed LEED patterns in Pd/Nb(110), Pd/Ta(110), and Co/Mo(110) systems. The energetics for Pd diffusion, island formation, and second to first adlayer atom incorporation are investigated.

I. INTRODUCTION

Experimental results concerning the structure, growth, and properties of transition-metal thin films have proliferated in recent years.[1] These thin-films, substrate systems are often found to exhibit transformations in their properties as a function of both coverage and temperature. The chemical and physical changes are particularly interesting for systems in which a late transition metal is deposited on an early transition metal. The chemical alterations are exemplified by modifications of the work function, hydrogen-uptake characteristics, and CO binding energies for systems such as Pd/Nb(110),[2–4] Pd/Ta (110),[5,6] Pd/W(110),[7] Co/Mo(110), and Co/Ni(110).[8]

It is unclear whether the effects observed are due to charge-transfer-induced changes in the nature of the adlayer or whether the effects are simply the result of lattice strain and phase transitions within the thin film. Considerable uncertainty also exists as to the mode of film growth, especially near the commensurate-incommensurate (CI) transition and at low deposition temperatures. We have undertaken a study, described below, which attempts to separate the structural and electronic effects, in order to discern which forces determine the observed structure and to elucidate possible growth morphologies for some of these thin-film systems.

This paper describes our results using a realistic model for the interactions involved in metal-on-metal thin-film growth. We have investigated the structure and growth mechanisms for Pd thin films on a bcc(110) substrate, at temperatures of 75 and 500 K and for Pd coverages ranging from 0.25 to 3.5 ML. The nature of the commensurate-incommensurate transition observed with this model is discussed in detail elsewhere,[9] but will be briefly summarized and expanded in this report.

An excellent illustration of the unusual nature of such films involves thin layers of Pd (a transition metal that adopts a fcc structure in the bulk) grown on W(110),[10] Nb(110), and Ta(110) (transition metals that have bcc bulk structures). Pick and co-workers[2,11] found that the addition of a single monolayer of Pd onto the surface of Ta or Nb greatly reduces the uptake of hydrogen into the bulk metal. For Pd coverages above one monolayer, the hydrogen uptake increases rapidly with film thickness up to that characteristic of bulk Pd. The electronic structure of these thin films of Pd is also greatly modified. Photoemission studies have shown that a single monolayer of Pd deposited on Nb(110) or Ta(110) has a 4*d* density of states similar to that of a noble metal (i.e., Ag), while a thicker Pd thin film that has recovered a near-bulk fcc(111) structure has a broader 4*d* band, similar to bulk Pd.[3] This perturbation in the electronic structure, toward a noble metal for the monolayer, is consistent with reduced hydrogen uptake as well, since H_2 does not dissociate readily on Ag experimentally.

The perturbed electronic structure is thought to be responsible for the changes in chemisorption properties of the film compared to the bulk. In addition to altered hydrogen absorption characteristics, Neiman and Koel[4] have used temperature programmed desorption to show that a single monolayer of Pd/Nb(110) has a CO binding energy of only ~ 0.43 eV, much lower than the binding energy of CO on bulk Pd(111) (1.3 eV). The experiments indicate that the binding energy can be continuously tuned over this range by controlling the thickness of the Pd film.[4,6]

In order to understand why the chemistry and electronic structure is altered at the surface of such a film, it is crucial to characterize the geometrical structure of the film as a function of Pd coverage and then to correlate changes in chemistry and electronic structure with morphology changes. Interesting structural questions arise from the deposition of a fcc metal on a bcc substrate and the implications this has on the competition between intralayer lattice strain and interfacial strain. Figure 1

shows the geometries for the bcc(110) and fcc(111) surfaces appropriate for Nb (or Ta) and Pd. A perfect $Pd_{fcc}(111)$ [defined here to be a Pd(111) layer with six equivalent nearest neighbors] overlayer on Ta(110) or Nb(110) has a lattice mismatch of only 2% along the bcc[$\bar{1}10$] direction, but this fcc film has an enormous mismatch of 18% along the bcc[001] direction. Since Pd has a fcc structure in the bulk crystal, a competition is immediately setup between the substrate and the bulk Pd structural preferences. For low Pd coverages on a bcc(110) substrate, the Pd atoms are thought to adsorb into a configuration commensurate with the underlying substrate lattice.[4,6,11,12] This structure minimizes interfacial strain but creates an internal strain within the Pd adlayer, since the Pd-Pd distances are expanded compared to the bulk. For multilayer coverages, the Pd film eventually forms a fcc lattice consistent with bulk Pd,[13] which minimizes the strain within the adlayer but potentially creates a large interfacial strain if the bcc(110) and fcc(111) lattices meet abruptly. Experiments indicate several distinct structural regimes for various coverages of Pd thin films on bcc(110) substrates.

A. Low coverage ($0.25 < \Theta_{Pd} < 1.00$ ML)

In this low-coverage regime, low-energy electron diffraction (LEED), and Auger-electron spectroscopy (AES) data suggest either pseudomorphic growth of a $Pd_{bcc}(110)$ layer [defined as a Pd(110) layer with four nearest neighbors and two next-nearest neighbors] or a completely disordered overlayer. Ruckman, Murgai, and Strongin[13] observe some extra LEED spots beginning to appear for $\Theta_{Pd} > 0.50$ ML but most experiments have yielded purely bcc(1×1) LEED patterns.[4,6,11,12] The extra spots may be caused by multiple-electron scattering from both the substrate and the adlayer, if the adlayer adopts an incommensurate structure. Such spots were observed also by Tikhov and Bauer for Co on Mo(110),[8] however mild annealing of the thin film recovered the perfect bcc(1×1) LEED pattern. Thus, for coverages below 1.0 ML, it is likely that the most stable structure is pseudomorphic $Pd_{bcc}(110)$.

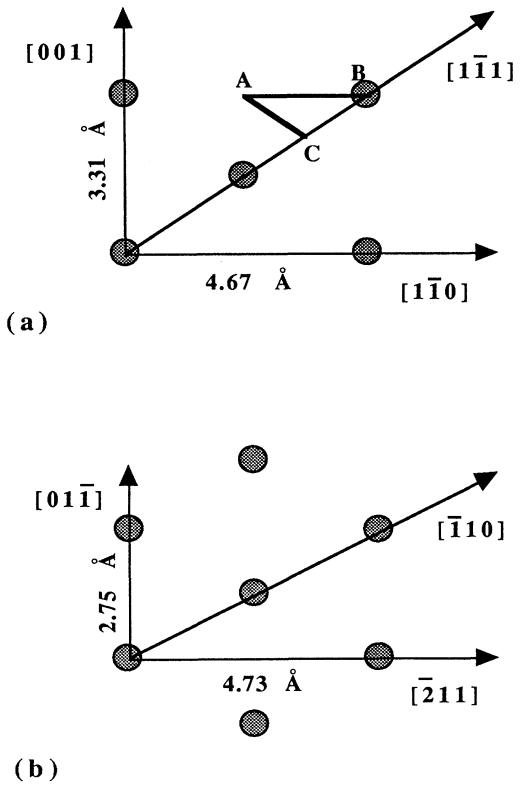

FIG. 1. The geometries of (a) a Nb(110) surface and (b) a Pd(111) surface, showing the lattice mismatch along the bcc[001] direction with the fcc[01$\bar{1}$] direction.

B. Intermediate coverages ($1.00 < \Theta_{Pd} < 1.50$ ML)

These are the coverages for which most of the experimental data suggest that some type of structural transformation occurs.[4,6,11,13,14] The primary indication of this phase transition is a change in the LEED from a bcc(1×1) to a more complicated pattern. During this transition, "beat patterns" or satellite spots in the LEED have been observed by two groups,[6,11,14] resulting in differing interpretations as to their origin. Strongin and co-workers[11,14] suggested that the spots arise from multiple scattering from the bcc(110) substrate and the fcc(111) adlayer. Koel, Smith, and Berlowitz[6] proposed an alternative possibility that some sort of ordered defect structure of Pd could form that would include both first and second adlayers. Strongin and co-workers[14] have also proposed that a first-order CI transition occurs, based upon the constant spacing between these beats in the LEED. A possible mechanism for this transition was discussed in an earlier paper using the present model.[9]

C. High coverages ($\Theta_{Pd} > 1.50$ ML)

For higher converges, growth has been proposed to proceed through a layer-by-layer (Frank-van der Merwe) growth mechanism[4,6] for several layers. This is based entirely upon AES measurements that show changes in the slope of the AES uptake curves at exposures thought to correspond to 2 and 3 ML. However, such changes in slope are somewhat controversial at these high coverages and hence other growth mechanisms may be operative. Eventually, the satellite spots undergo a gradual decrease until the LEED pattern is fully fcc(1×1).[8,13]

The majority of experimental studies of Pd films on Nb(110) and Ta(110) were performed at high surface temperatures (500–1100 K). Studies of Co/Mo(110) and Ni/Mo(110) show that temperature can have a large effect on both the structure and work function of these thin layers.[8] Therefore, the growth mode and any phase transitions at low temperatures may be quite different from that for high-temperature thin-film growth.

As we have outlined, the structure of thin films of fcc metals on bcc substrates can change drastically as a function of temperature and coverage and both the identity and the cause of the observed structures are still contro-

versial. The primary focus of our theoretical work is to understand the effect of this tremendous interfacial strain, caused by the large lattice mismatch of the ideal $Pd_{fcc}(111)$ film and the bcc(110) substrate, on the structure of the deposited film.

Several theoretical studies have shown that a fcc(111)/bcc(110) interface can minimize its interfacial strain by adopting an optimal orientation at the boundary.[15–19] This optimal orientation can be predicted based purely on the lattice constants of the bcc and fcc crystals forming the interface. Paik and Schuller[19] have also attempted to include temperature effects in their model by using perturbation methods. Based upon these models, the present system is predicted to adopt the Nishiyama-Wasserman (NW) orientation at the interface,[16] in which the fcc[01$\bar{1}$] direction is parallel to the bcc[001] direction (see Fig. 1). The drawback of these previous models is that both the substrate and adlayer were held rigidly in their respective bulk lattice positions and only the relative orientation was optimized.

The relief of interfacial strain has been examined using surface dislocation models in which the distribution of burgers vectors on the surface is adjusted,[20] but this model is unable to give quantitative descriptions of the interfacial structure. McTague and Novaco have shown that some of the interfacial strain may be relieved by the formation of mass density waves at the interface, caused by misfit dislocations.[21] In order to explore the mechanisms for the structural changes and to predict structures as a function of coverage, we have gone beyond previous models by abandoning the rigid lattice approximation for the adlayer[9] and by explicitly examining the effect of temperature.

II. THEORETICAL MODEL, SIMULATION METHOD, AND MODES OF ANALYSIS

We model the Pd adlayer-substrate system with the Pd embedded-atom method (EAM) potential of Foiles, Daw, and Baskes.[22] This empirical potential formulates the energy of interaction for a metal, E_{tot}, in terms of short-ranged, repulsive, two-body interactions, $\phi(R_{ij})$, which are meant to represent the core-core repulsion, and an embedding energy, $F_i(\rho)$, that represents the energy to embed an atom i into a background electron density, ρ:

$$E_{tot}=\sum_i F_i(\rho)+\tfrac{1}{2}\sum_{i\neq j}\phi_{ij}(R_{ij}) \ . \tag{1}$$

The electron density at a point in the system is found by a superposition of atomic densities

$$\rho=\sum_{j\neq i}\rho_j(R_{ij}) \ . \tag{2}$$

F_i and $\phi(R_{ij})$ are fit to experimental data such as the cohesive energy and elastic constants of the bulk crystal and are represented as numerical functions of R_{ij}.

This potential has been shown to reproduce the bulk and surface properties of Pd reasonably well. More generally, the EAM potential has been used in studies of the critical thickness of thin fcc(111)/fcc(111) films by Dodson[23] and by Wolf[24] in studies of the elastic properties of thin slabs. The results of these studies substantiate the use of the EAM potential for thin films. Some bcc EAM potentials have been constructed, including one for Nb,[25–28] but no potentials have been developed for bcc/fcc alloys such as Pd/Nb or Pd/Ta. Thus, we instead use a simpler model of the substrate-adlayer system, which we now describe.

We have chosen to model the bcc substrate by placing fixed Pd atoms at bcc(110) lattice sites, with a lattice constant of 3.31 Å. Since Ta and Nb are bcc metals with nearly identical lattice constants (3.30 and 3.31 Å), our model is meant to represent the bcc(110) corrugation for both metal substrates. We therefore retain the rigid lattice approximation for the substrate, but release this constraint for the adatoms, allowing them to move under the influence of the adatom-substrate and adatom-adatom interactions. By using identical potentials for both the intralayer and interlayer interactions, our model neglects substrate-adlayer charge transfer that may modify the nature of the Pd-Pd, substrate-substrate, or Pd substrate interactions. Importantly, neglect of such electronic effects allows us to address the effect of lattice strain alone on film structure. The use of this approximation for the adatom-substrate interactions is partially justified by the fact that the predicted Pd binding energies on this substrate are in reasonable agreement with experimentally determined Pd/Ta(110) binding energies (discussed below). If experiments for Pd on Nb(110) and Ta(110) yield similar results to our model, then lattice strain relief is probably the dominant driving force for the structural changes in these systems.

Four fixed layers of this bcc(110) structure were used to simulate the substrate in a two-dimensional periodic slab that had 14×14 bcc(110) surface unit cells, leading to a simulation cell size of 65.53×46.34 Å^2 with 392 atoms per substrate layer. The size of the periodic cell was chosen because it induces only a 0.92% compression in a perfect $Pd_{fcc}(111)$ layer along the bcc[001] direction. This is a distortion of only 0.025 Å for the fcc Pd—Pd bond lengths along the fcc[01$\bar{1}$] direction. Along the bcc[1$\bar{1}$0] direction, a compression of 1.80% is present in a perfect fcc adlayer. This compression in the fcc[$\bar{2}$11] could only be relieved by using a periodic box that is narrower in the bcc[1$\bar{1}$0] direction. The overall effects of these boundary-induced strains on the results presented here were tested by performing simulations on various-sized periodic cells with varying compressive or expansive strains induced in the adlayer. The boundary-induced strains that were found have little or no effect on the types of structures present over the entire coverage range examined.

Monte Carlo (MC) and molecular dynamics (MD) simulations (both constant *NVT* and constant *NVE*, where N denotes the number of particles, V denotes volume, E denotes total energy, and T denotes temperature) were performed for a range of coverages (0.25–3.50 ML) and temperatures (75–1000 K). For the high-temperature studies ($T\leq500$ K), the Pd thin films were deposited in the variety of ways in order to attain maximum equilibration and the ensure that widely varying regions of configuration space were investigated. For cov-

erages below 1.00 ML, adatoms were distributed randomly in a 0.4-Å thick slab, which was centered 2.0 Å above the substrate surface [for comparison, the interlayer spacing in Ta(110) is 2.34 Å]. The adatoms were then equilibrated for up to 50 000 MC steps/adatom at the desired temperature. Variable length maximum displacements between 0.3 and 2.8 Å were used to enhance equilibration of the adlayer. For coverages above 1.00 ML, the thin film was allowed to grow under a Monte Carlo deposition scheme in which a Pd atom was deposited approximately 2.0 Å above the topmost Pd layer, every 50 000–200 000 MC steps. This allowed some equilibration between each adatom addition. Once a desired coverage was generated, the thin film was thoroughly equilibrated for 8–16 million MC steps before the structural and energetic properties were investigated. For the low-temperature studies ($T=75$ K), the entire film was generated by the MC deposition process, starting from zero coverage. MD trajectories[29] of up to 150 ps in length were used to test for full equilibration and the results were compared to the MC simulations. In this manner, we could allow large scale cooperative behavior that might be needed to achieve full equilibration.

The underlying potential minima for these equilibrated structures were examined by cooling the adatoms to 0.1 K via both slow stepwise cooling and fast quenches. The stepwise cooling involved equilibrating the adlayer at 500, 400, 300, 200, 100, and 0.1 K. If thorough equilibration is achieved at each of the successive temperatures, then the system should find a minimum energy configuration that is close to the global energy minimum. The fast quench was achieved by selecting instantaneous, equilibrated configurations and changing the temperature to 0.1 K. If the jump steps are fairly small (0.1 Å) for these quenches, then the system will drop into the nearest local minimum in the potential energy surface.

Once the structure was equilibrated at each of these coverages, four different probes were used to characterize the structure of these films. First, both radial and angular distribution functions were analyzed for all adatoms. The radial distribution function is defined here without the usual division by the bulk density, since defining a density at the surface of this system is not unique. The angular distribution function, $g(\theta)$, is constructed by finding all neighbors of each atom within a radial cutoff (3.50 Å) and calculating all of the angles between these atoms, normalized by the total number of atoms in the adlayer. Our standard point of reference, the perfect $Pd_{bcc}(110)$ commensurate overlayer, exhibits a radial distribution with a nearest-neighbor (NN) peak at 2.86 Å and next-nearest-neighbor (NNN) peaks at 3.31 and 4.68 Å. The angular distribution has peaks at 54.6°, 70.7°, 109.3°, 125.4° and 180.0°. By contrast, the perfect $Pd_{fcc}(111)$ adlayer (with $a_0=3.89$ Å) exhibits radial distribution peaks at 2.75 Å (NN) and 4.73 Å (NNN) and angular distribution peaks at 60°, 120°, and 180°. Another structural analysis tool that we employed involved construction of bond network diagrams for the thin film. If a line is drawn between all atoms less than 3.1 Å apart, those atoms in a bcc(110) configuration will have four lines attached and those in a fcc(111) configuration will have six lines. This allows the various domains of fcc- and bcc-like regions to be readily identified. Finally, we also calculated the two-dimensional structure factors, $S(k)$, for comparison to LEED patterns observed for these films.

III. RESULTS

A. High-temperature growth ($T=500$ K)

The low-coverage results ($\Theta_{Pd}<1.25$ ML) have been discussed elsewhere.[9,30] Briefly, Pd thin-film growth below 1.0 ML is found to be fully pseudomorphic and favors the formation of two-dimensional islands. For example, at 0.50 ML a single equilibrated bcc island is 0.04 eV/adatom lower in energy than an equilibrated set of dispersed anisotropic islands and 0.35 eV/adatom lower in energy than a single fcc island.[9,30] Figure 2 shows angular and radial distributions at 0.75 ML for a configuration slowly cooled to 0.1 K. Both of these strongly suggest that the adlayer is primarily bcc at this coverage. Notice that $g(\theta)$ has minima at the fcc hexagonal angles of 60° and 120° and $g(r)$ has a well-resolved second-neighbor peak near 3.3 Å, with the first peak slightly contracted to 2.67 Å. At $\Theta_{Pd}=1.0$ ML, the most stable structure is a fully commensurate adlayer, however we find that defects can form at finite temperatures. These defects cause a few locally fcc regions to form. Upon cooling to 0.1 K, pseudomorphic structures with a few defects are found to be local minima on the potential

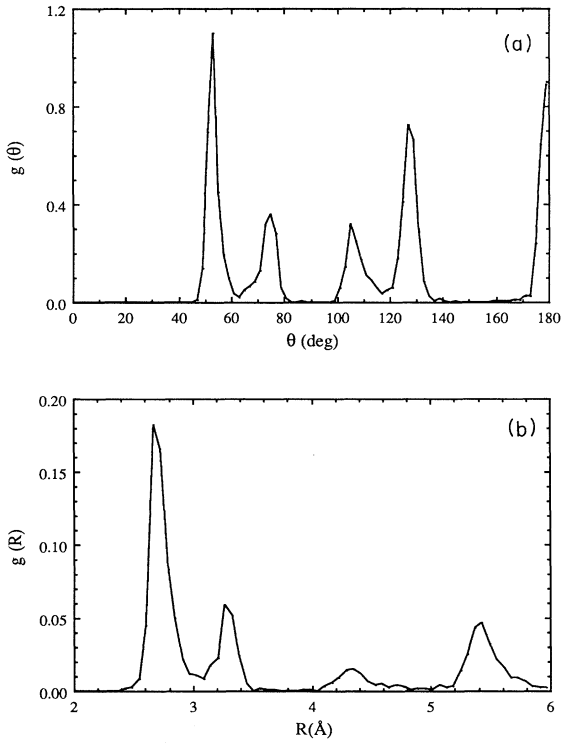

FIG. 2. The $g(\theta)$ and $g(r)$ distribution functions for a slowly cooled configuration at $\Theta_{Pd}=0.75$ bcc ML.

energy surface that are higher in energy than the global minimum by energies of only ~0.012 eV/adatom.

We find the average adatom binding energy at submonolayer coverages to be approximately 3.90 eV/adatom for the slowly cooled structures at 0.1 K. This is close to the bulk cohesive energy of Pd (3.91 eV for both the EAM potential and experiment). Temperature programmed desorption experiments of Koel and Smith[6] of Pd/Ta(110) find the average binding energy at submonolayer coverages to be approximately 4.2±0.2 eV/adatom. Thus, we see that the substrate-adatom energetics in this model are reasonably representative of the true substrate-adatom interactions.

We have also explored the potential energy surface for motion of a lone Pd atom on the bcc(110) substrate. The potential is very flat in the bcc[1$\bar{1}$0] direction about the pseudomorphic site, allowing considerable distortions at a small cost in energy, consistent with the contracted Pd-Pd distances in the radial distribution function (Fig. 2). For example, moving 0.70 Å along the bcc[1$\bar{1}$0] direction away from the pseudomorphic site only raises the energy by 0.1 eV/adatom. The energy barrier for diffusion along a path between pseudormorphic sites [$A-C$ in Fig. 1(a)] in the [1$\bar{1}$1] direction is found to be 0.41 eV. Diffusion between pseudomorphic sites along the [1$\bar{1}$0] direction, which involves passing directly over a substrate atom [$A-B$ in Fig. 1(a)], has a barrier of 1.08 eV. In contrast, we find lower energy barriers (0.3 eV/adatom) for diffusion of Pd adatoms that remain attached to the edge of existing $Pd_{bcc}(110)$ islands. Previous results indicate that this small barrier gives rise to diffusive motion of Pd island edges allowing them to be reshaped easily, leading to Pd islands that grow preferentially along the bcc[001] direction. This anisotropic growth of islands occurs because this maximizes the number of nearest-neighbor plus next-nearest-neighbor attractive interactions.[30]

We predict that a CI [$Pd_{bcc}(110) \rightarrow Pd_{fcc}(111)$] transition occurs at coverages between 1.0 and 1.25 bcc ML. The transition occurs without the formation of a second distinct Pd adlayer. The mechanism for this phase transition involves immediate incorporation of atoms that are deposited above the pseudomorphic Pd adlayer into the first layer.[9] A very similar transition has recently been experimentally observed for Co/Mo(110) and Ni/Mo(110).[8] In our simulation, the incorporation of adatoms into the first layer causes the formation of fcc(111) and bcc(110) domains that appear stable if deposition is halted. Figure 3 shows radial and angular distributions at 1.10 ML and Fig. 4 shows the bond network diagram for this coverage. The formation of additional peaks in both $g(\theta)$ (at 60° and 120°) and $g(r)$ near 2.6 Å, while maintaining the bcc peaks, indicate the presence of both $Pd_{bcc}(110)$ and $Pd_{fcc}(111)$ domains. The bond network in Fig. 4 supports this assignment as well, with regions where atoms have six neighbors (fcc) coexisting with regions where atoms have only four neighbors (bcc).

The fcc domains continue to grow as the coverage is increased. Figure 5 shows that at $\Theta_{Pd}=1.75$ ML, the $g(\theta)$ peaks are now centered at 60° and 120° and the radial distribution function no longer shows a second-

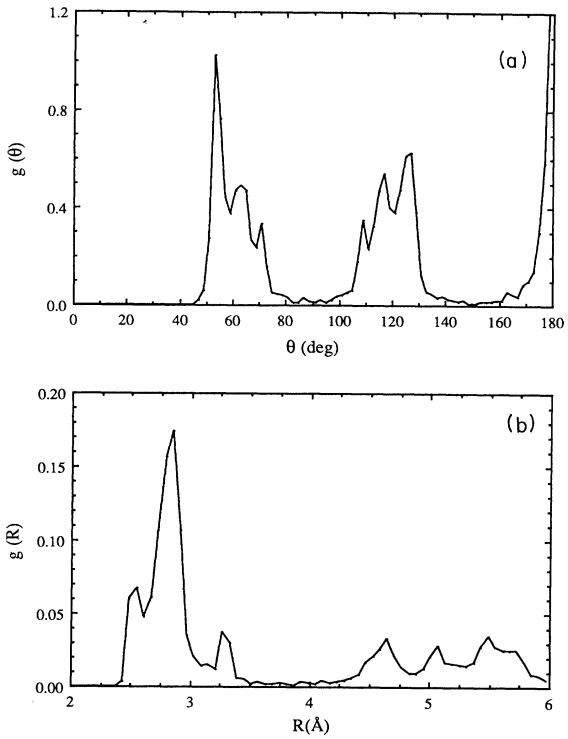

FIG. 3. The $g(\theta)$ and $g(r)$ distribution functions for a slowly cooled configuration at $\Theta_{Pd}=1.10$ bcc ML.

neighbor peak at 3.31 Å. Thus, the second layer as well as the first layer are now in a fcc arrangement. From $\Theta_{Pd}=1.25-3.50$ bcc ML, growth continues in a structure that is predominantly $Pd_{fcc}(111)$, with no trace of the commensurate structure remaining in either the radial or angular distribution functions. At these coverages the adlayer has an overall Nishiyama-Wasserman orientation (fcc[01$\bar{1}$] parallel to the bcc[001]) that is somewhat perturbed by transverse two-dimensional wavelike distortions that propagate in the bcc[001] direction.

These wavelike distortions first appear during the CI

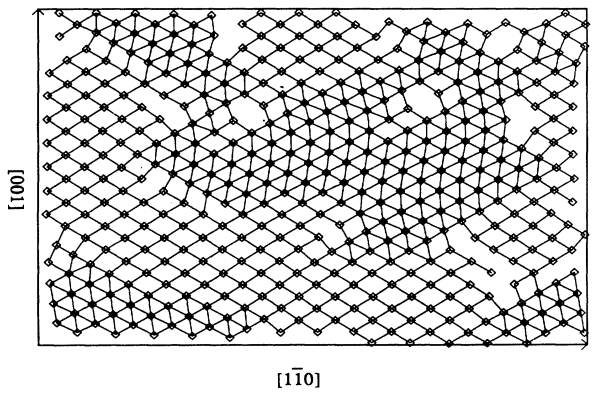

FIG. 4. A bond network diagram for $\Theta_{Pd}=1.10$ bcc ML, exhibiting distinct regions of fcc- and bcc-like bonding.

transition and are fully developed in the first adlayer once it has been converted completely to a close-packed layer. We suspected that these waves might represent the "ordered defect structure" suggested by Koel, Smith, and Berlowitz[6] and that they might cause the curious beat patterns observed in LEED. In order to characterize these structural changes further, we simulated a LEED pattern for each layer of the Pd thin film by computing a two-dimensional structure factor

$$S(k_x,k_y)=\frac{1}{N^2}\sum_{i}^{N}\sum_{j}^{N}\exp^{-i(k_x x_{ij}+k_y y_{ij})}, \quad (3)$$

where $x_{ij}=x_i-x_j$ and $y_{ij}=y_i-y_j$ for each particle i and j in the adlayer. Figure 6 shows the primary peaks in the structure factor for perfect $Pd_{bcc}(110)$ and $Pd_{fcc}(111)$ planes [Figs. 6(a) and 6(b), respectively], where we see that they can be distinguished by the perfect hexagonal symmetry of the fcc(111) pattern as compared to the distorted hexagon of the bcc(110) pattern. Figure 7(a) depicts the predicted structure factor of the first adlayer for an equilibrated 1.75 bcc ML film. We find that these extra spots around the primary fcc spots are due to these two-dimensional waves. This is shown easily in two independent ways: (i) by taking a perfect fcc overlayer characterized by the $S(k)$ shown in Fig. 6(b), deliberately inducing a wave in it, and calculating its structure factor; and (ii) by relating the difference in wave vector, δk, to the wavelength of the distortions. Inducing a wave with $\lambda=15$ Å yielded the same type of structure factor observed in Fig. 7(a). Thus the waves change the LEED pattern from a perfect fcc or bcc symmetry to a lower symmetry pattern characteristic of the length of these two-dimensional waves. Second, the difference in wave vector δk between spots in Fig. 7(a) predicts a wavelength of 15.4 Å, while the wavelength observed in the real-space image of the first adlayer [Fig. 7(b)] is ~15 Å. Similar differences in wave vectors are observed experimentally, corresponding to wavelengths of approximately 17 Å (Ref. 14) and 23 Å.[13] This similar spot spacing in theory and experiment suggests that these structural waves in the $Pd_{fcc}(111)$ layer are probably the source of the strikingly similar LEED beat patterns. We emphasize that this analysis does not involve multiple-electron scattering from the adlayer and substrate, which has been a common interpretation of the beats observed experimentally.[11,14]

The structural waves are formed in an attempt to relieve some of the interfacial strain at the bcc(110)/fcc(111) interface. Figure 8 depicts the way in which this interfacial strain is relieved, as illustrated in two bond network diagrams, where atoms are located at each vertex. Figure 8(a) represents a perfect fcc(111) layer superimposed on a perfect bcc(110) layer. The system

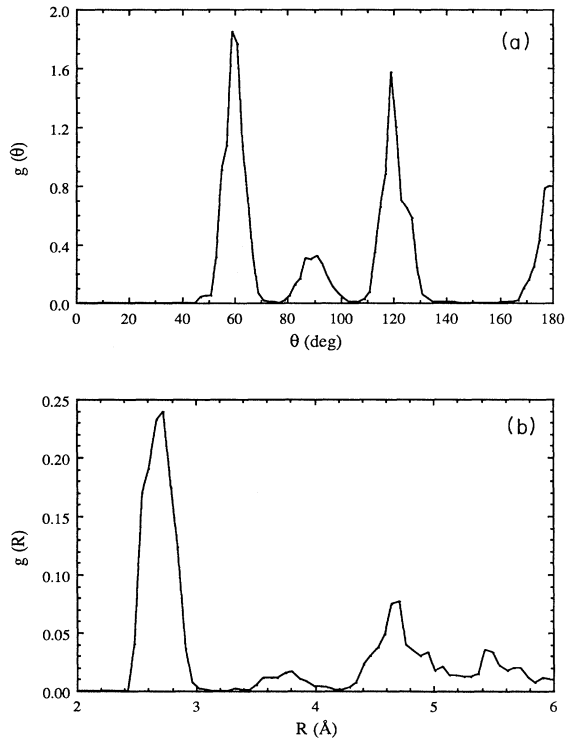

FIG. 5. The $g(\theta)$ and $g(r)$ distribution functions for a quenched configuration at $\Theta_{Pd}=175$ bcc ML.

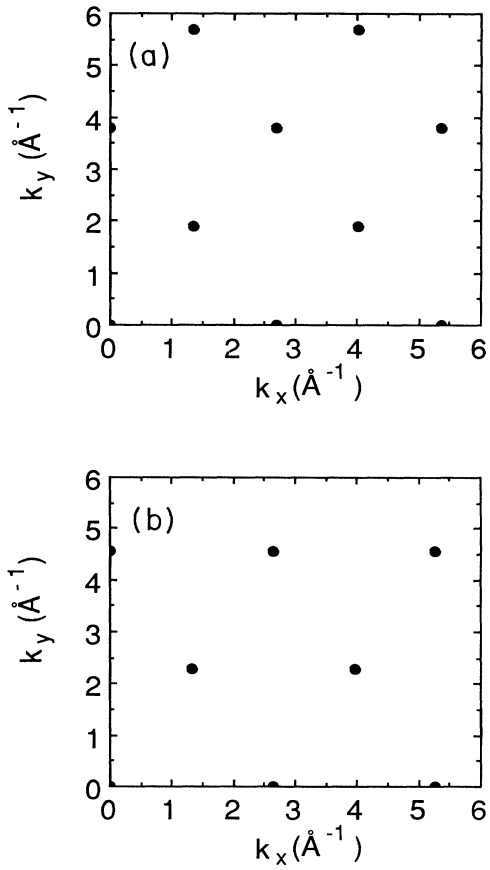

FIG. 6. The structure factor $S(k)$ for (a) a perfectly pseudomorphic $Pd_{bcc}(110)$ adlayer and (b) a perfect $Pd_{fcc}(111)$ adlayer.

has misfit dislocations where adatoms are forced to lie directly above substrate atoms approximately every 16–18 Å in the bcc[001] direction. A similar bond network in Fig. 8(b) depicts the equilibrated thin film at $\Theta_{Pd}=1.50$ ML. Virtually nowhere are adatoms directly above substrate atoms. Therefore, these waves spread the strain due to the misfit dislocation evenly over the entire adlayer. The precise structure of the distortions can be seen in an expanded view of the substrate and adlayer. Figure 9 shows the adlayer and substrate atoms in which the wavelength of the distortion is seen to be ~15 Å and the amplitude is ~0.35 Å. This is consistent with the earlier result that the potential energy surface is very flat for distortions of a lone Pd adatom along the bcc[1$\bar{1}$0] direction. In a close-packed layer of adatoms, the near-neighbor interactions with other Pd adatoms will offset some of the energy cost for such distortions.

We find that the waves diminish rapidly away from the interface. For example, at 3.3 bcc ML, the second adlayer is almost fully formed and essentially no waves are present in this second layer [Fig. 10(a)]. In particular, we find that the satellite peaks in the structure factor diminish with layer thickness, until the pure fcc structure factor is all that is observed for the topmost adlayer [Fig. 10(b)]. This is completely in accord with LEED observations of a gradual disappearance of the beat pattern, which is replaced by a fcc(1×1) diffraction pattern.

Finally, the higher coverage growth (>1.5 bcc ML) does not occur in a strictly layer-by-layer fashion. When

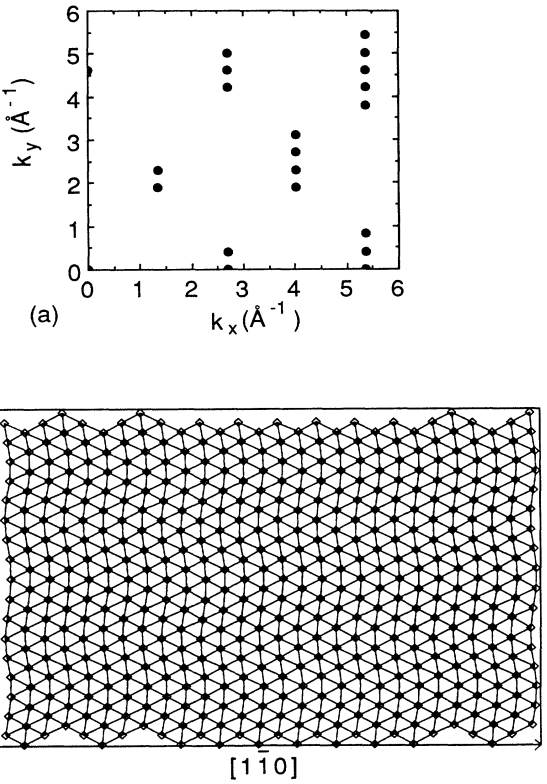

FIG. 7. (a) The structure factor, $S(k)$, and (b) its corresponding bond network diagram for the first Pd adlayer at a total coverage of 1.75 bcc ML and $T=500$ K.

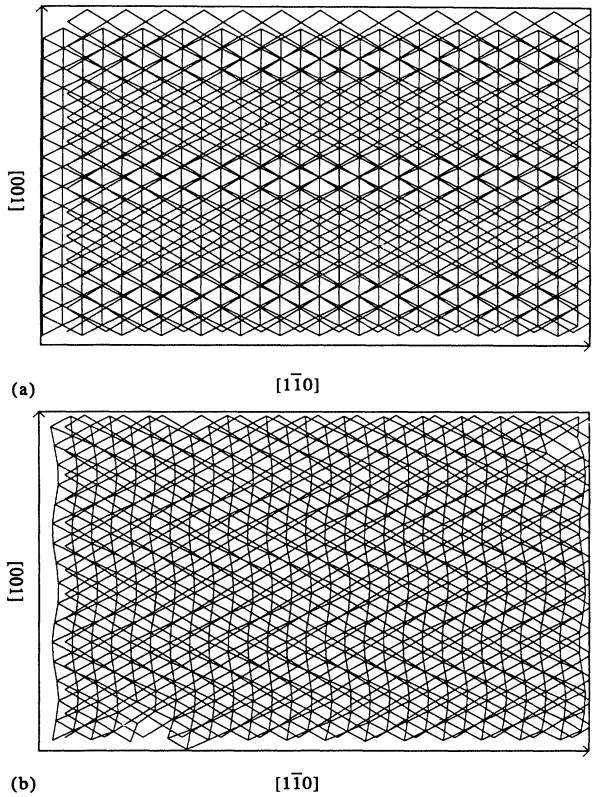

FIG. 8. Bond network diagrams for (a) a perfect Pd fcc(111) adlayer atop a perfect Nb bcc(110) substrate; (b) the first adlayer of 1.75 bcc ML Pd adsorbed on a Nb bcc(110) substrate, equilibrated by MC deposition at $T=500$.

MC deposited atoms land above a close-packed fcc region, they cannot be incorporated into the lower layer. The only mechanism for layer-by-layer growth would then involve diffusion to steps. The energy barriers for diffusion of a single second-layer Pd adatom above a

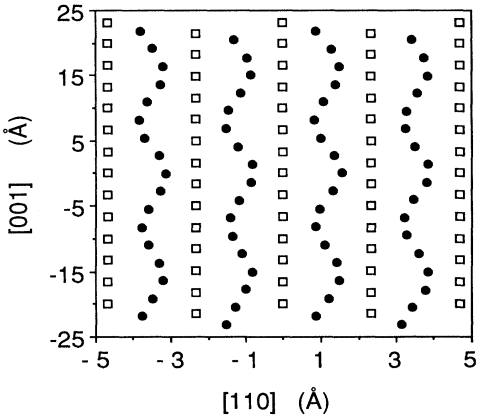

FIG. 9. An expanded view of the wavelike distortions present in the adlayer. This is the structure of the substrate and first adlayer for a 1.75 bcc ML coverage cooled to 0 K. The substrate atoms are represented by open squares and the adatoms by solid circles.

$Pd_{fcc}(111)$ monolayer are small (~ 0.15 eV), but once second-layer islands begin to form then diffusion of a single atom away from the island involves a considerable energy barrier. For this reason, the film appears to grow in a three-dimensional manner, with up to three incomplete adlayers atop each complete adlayer. This is reminiscent of Stranski-Kranstov film growth, rather than Frank-van der Merwe growth.

B. Low-temperature growth

The tremendous instability of the pseudomorphic $Pd_{bcc}(110)$ adlayer at 500 K for coverages above 1 bcc ML led us to investigate the structure and growth mode of these Pd thin films at lower temperatures. At very low temperatures, diffusion will be hindered, yet the barrier to incorporation of a second-layer atom into a pseudomorphic first layer may be small enough to be accessible. If this barrier is small, incorporation will occur and incommensurate growth may result, even at low temperatures.

The Pd thin films were generated by random MC deposition onto the rigid substrate at a temperature of 75 K. In contrast to the high-temperature deposition case, we find that a pseudormorphic overlayer is stable at 75 K, even up to 2.1 ML. The adatoms in the second layer are not incorporated into the first layer using either MC or MD simulations with very long equilibration times. Figure 11 shows the bond network diagram for the first and second adlayers at a total coverage of 2.1 ML. The growth is seen to be three-dimensional as well as pseudomorphic. Some local areas of higher coordination may indicate the early stages of transformation to the fcc film, but these areas never reached a critical nucleation size during our simulations.

We compared the 0 K energy of $Pd_{fcc}(111)$ structure at 1.25 bcc ML with the 0 K energy of a completely pseudomorphic $Pd_{bcc}(110)$ structure at the same coverage. The $Pd_{fcc}(111)$ thin film was found to be lower in energy by 0.33 eV per adatom. Thus, it appears that the pseudomorphic thin film found at 75 K is only metastable with respect to transformation to a fcc structure. To study the metastability of this phase, we performed long MC and constant temperature MD (Ref. 31) equilibration runs at 75 K. The structure did not change qualitatively during these simulations (~ 8 million steps for MC and ~ 150 ps for MD). We then performed MC simulations, on the 1.5-ML pseudomorphic film, where we raised the temperature in 50 K increments and equilibrated at each temperature. Interestingly, the metastable bcc phase remained even upon raising the temperature to 325 K. At this temperature we began to see occasional interdiffusion of Pd adatoms from the second layer to the

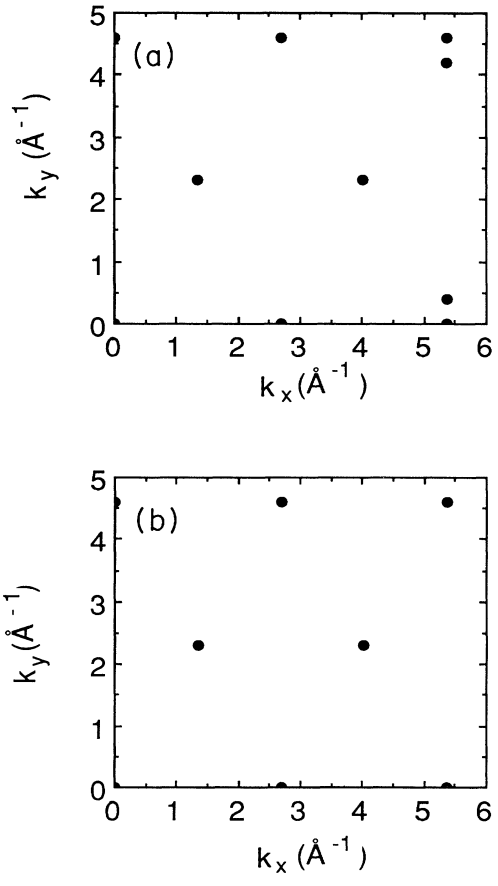

FIG. 10. The structure factors $S(k)$ for (a) the second layer and (b) the third layer of 3.3 bcc ML film deposited at 500 K.

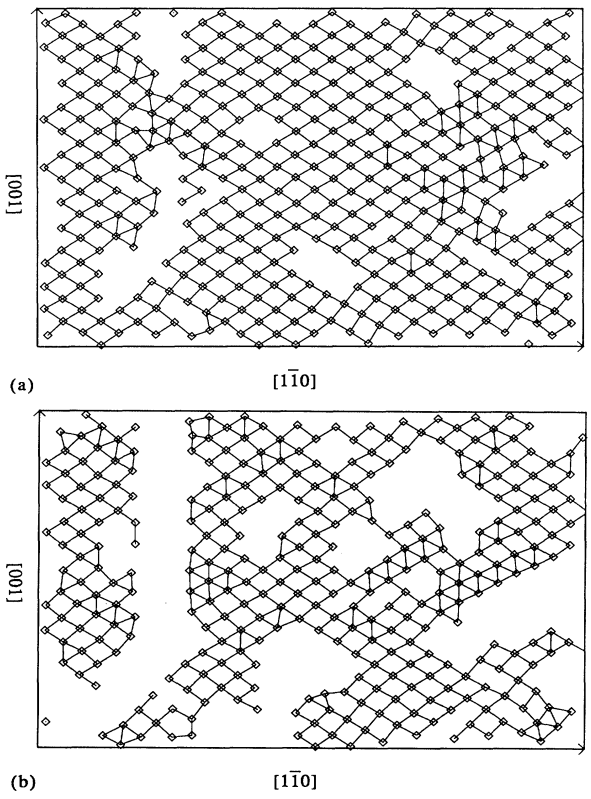

FIG. 11. The bond network at a total coverage of 2.1 bcc ML at 75 K: (a) the first adlayer and (b) the second adlayer.

first. We were unable to run simulations long enough to achieve a full phase transition in the first adlayer, at this temperature, but we feel that 325 K represents the approximate limit to the metastability of the pseudomorphic film for this coverage.

This prediction of metastability for the pseudomorphic structures prompted us to investigate the energy barrier for incorporation of a second-layer atom into the first adlayer in a more systematic fashion.[30] We constructed an 18-adatom, two-dimensional cluster in pseudomorphic positions on the surface. An additional adatom was brought slowly toward the center of the cluster in steps of 0.1 Å. At each step, a steepest descent minimization (relaxation) of the 18-atom cluster was performed. Figure 12 shows the cluster and the two positions for which this analysis was performed. The approach at site *A* is where a perfectly pseudomorphic second-layer atom would reside and site *B* is between rows of substrate atoms. Figure 13 displays the potential energy curves for the two approaches, where we see that a second layer pseudomorphic site is stable, but that an incoming atom that is able to push between atoms in the cluster at site *B* will find an energetically favorable location as well. The barrier between a pseudomorphic second-layer site and an incorporated first-layer site is shown to be about 0.4 eV in this static analysis. This barrier is due to the diffusion of the Pd from *A* to *B*, while remaining in the second layer. Once the Pd adatom is above site *B* there is no barrier to incorporation. Of course, it is possible that the vibrational motion of the first-layer atoms will lower this diffusion barrier significantly, but this analysis indicates that a substantial diffusion barrier still exists and may be responsible for the kinetically stabilized pseudomorphic film formed by deposition at 75 K.

IV. DISCUSSION AND CONCLUSIONS

The results presented here for growth and structure of Pd thin films on a bcc substrate can be used to interpret the wide and sometimes contradictory range of experimental information for Pd/Nb(110), Pd/Ta(110), and even Co/Mo(110). The structure of submonolayer films and the commensurate-incommensurate transition are reported elsewhere,[9] but some brief discussion of these results is useful.

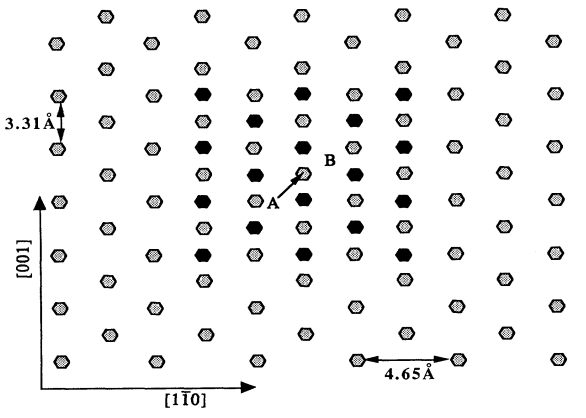

FIG. 12. The 18-adatom pseudomorphic bcc cluster (black hexagons) and the top layer of substrate atoms (grey hexagons) are shown. Position *A* is directly above a substrate atom and *B* is located between both substrate an adatom positions.

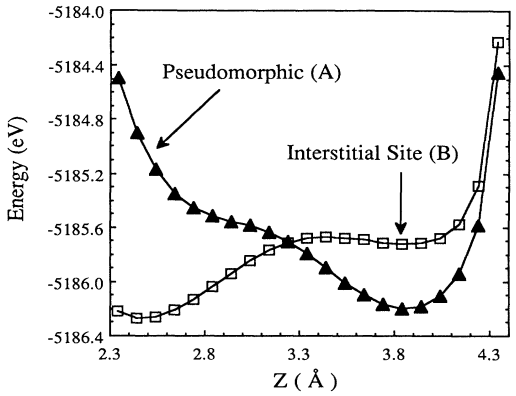

FIG. 13. The potential energy curves for the two approaches of an additional Pd atom toward the 18-adatom cluster of Fig. 12. The abscissa is the surface normal distance, z (Å), of the approaching atom from the top layer of fixed substrate atoms. A z value of 3.8 Å corresponds to a second adlayer atom and a z value of 2.4 Å corresponds to a first adlayer atom.

At 500 K, the growth mode depends sensitively upon the coverage. For submonolayer coverages, pseudomorphic bcc adlayer islands are always more stable than fcc islands. Artificially constructed fcc islands are observed to transform to bcc islands spontaneously. The islands grow preferentially along the bcc[001] direction in order to maximize the number of nearest and next-nearest-neighbor interactions.[30] Such preferred directions for island growth that lead to long-range channels on the surface, as well as the predictions of $g(\theta)$ as a function of Θ_{Pd}, should be directly comparable to ion scattering experiments.

The periodic corrugation potential of the substrate is found to determine the preferred growth geometries at these coverages, consistent with the bcc(1×1) patterns observed by LEED for systems such as Pd/Nb(110) (Refs. 11 and 14) and Pd/Ta(110).[6] Satellite spots in the LEED are seen for submonolayer coverage of Pd/Ta(110) (Ref. 13) and Co/Mo(110).[8] These were interpreted by Tikhov and Bauer to be caused by incorporation of second-layer adatoms into the first adlayer, causing a local transformation to a close-packed adlayer structure.[8] This interpretation is in complete accord with our simulation results, where indeed local fcc regions are formed. It is also consistent with our calculations of a relatively low (0–0.4 eV) energy barrier for incorporation of a second layer adatom into the first adlayer.

The bcc-to-fcc transition is found to occur for coverages between 1.0 and 1.20 bcc ML. This transition relieves the large intralayer strain within the pseudomorphic adlayer caused by expanded Pd—Pd bonds. The transition mechanism involves the formation of stable fcc and bcc domains within the first adlayer. The fact that we see stable, separate domains provides evidence that the CI

structural transformation for this model system involves a first-order phase transition and lends credence to an earlier proposal that the CI transitions for Pd/Nb(110) and Pd/Ta(110) also occur via such a transition.[14] This coexistence of fcc and bcc regions could give rise to the satellite spots in the LEED observed at these coverages, if a multiple-electron scattering mechanism is invoked.

For coverages above 1.25 bcc ML, the fcc adlayer structure is lower in energy than pseudomorphic bcc structures at the same coverage. At these coverages, the calculated and experimental LEED pattern due to the bcc substrate diminishes, replaced by a complex beat pattern. We predict that this pattern is due to the fact that the $Pd_{fcc}(111)$ adlayer is not fully ordered, and relieves strain due to misfit dislocations at the bcc/fcc interface by forming wavelike distortions in the adlayer. These atomic distortions result in satellite spots in our calculated structure factor, similar to those observed in LEED at the same coverages.[6,8] If this is the cause of the satellite spots, then the central spots should have a symmetry close to that of a fcc(111) adlayer. The second adlayer is found to form a structure with less pronounced wavelike distortions that diminish as the second layer becomes complete. If the extra LEED spots are caused by the waves, they should also diminish as the second layer forms. Indeed, we find few extra spots in the structure factor for the second and third epitaxial layers, with the characteristic fcc(1×1) pattern appearing instead, completely consistent with LEED observations.[4,6,8,11,13,14]

This suggestion that structural waves may cause satellite spots at misfit interfaces needs to be investigated experimentally. One way of distinguishing between multiple-electron scattering and structural wavelike distortions as sources of beat patterns would be to use an experimental probe sensitive only to the topmost layer (eliminating the multiple-scattering channel). Helium scattering or grazing incidence x-ray diffraction are possible tools for testing our prediction. If the beats remain in these two diffraction experiments, this provides strong evidence for our structural assignment.

Thin-film growth appears to be quite different for the low (75 K) and high (500 K) temperature regimes. At low temperatures, pseudomorphic growth is found to be stable up to adlayer coverages of 3.5 bcc ML. The growth is found to be three dimensional due to the low rate of both interlayer and intralayer diffusion. Up to three incomplete Pd adlayers are found to be forming on top of the completed adlayers. The prediction of a kinetically stabilized bcc phase of Pd via growth at low temperatures is an intriguing possibility for experimentalists to investigate. Such bcc Pd films should have very different properties from fcc films, perhaps being more reactive due to their more open structure. Experimental studies to date have only grown Pd thin films at 300 K and above. Our results for low-temperature growth seem to indicate that pseudomorphic growth of more than 1 ML of Pd onto a cold bcc(110) substrate is possible and may be stable at least up to room temperature. An extremely cold source of Pd atoms and a cold substrate would have to be used in order to keep the adlayer film at low temperature.

Thin film growth at such fcc/bcc interfaces involves a competition between the substrate corrugation potential that favors pseudomorphic growth and the internal strain in the commensurate adlayer, which prefers a fcc(111) structure. We find that the competition between interfacial and intralayer strains determines the observed structural changes, resulting in the formation of incommensurate films at 500 K and metastable pseudomorphic films at very low temperatures. Since this empirical EAM potential that ignores electronic effects of the chemically heterogeneous interface predicts similar structural changes to those found in the actual Pd/Nb(110), Pd/Ta(110), and Co/Mo(110) thin layer systems, we conclude that lattice strain and diffusional barriers are the key players in determining the structure of these thin films at various coverages and temperatures.

ACKNOWLEDGMENTS

This work is supported by the Office of Naval Research (Grant No. N00014-89-J-1492). E.A.C. also acknowledges partial support from the National Science Foundation and the Camille and Henry Dreyfus Foundation. We thank Dr. S. Foiles for providing the embedded-atom-potential data for Pd and Professor B. E. Koel for helpful discussions. Simulations were performed on an FPS Model 500 obtained through support from the Department of Defense University Research Instrumentation Program (Grant No. N00014-89-J-1378).

[1]E. Bauer, *Metals on metals,* Vol. 3B of *Chemical Physics of Solid Surfaces and Heterogeneous Catalysis,* edited by D. A. King and D. P. Woodruff (Elsevier, Amsterdam, 1984), Chap. 1, pp. 1–57.

[2]M. A. Pick, J. W. Davenport, M. Strongin, and G. J. Dienes, Phys. Rev. Lett. **41**, 286 (1979).

[3]M. El-Batanouny, M. Strongin, G. P. Williams, and J. Colbert, Phys. Rev. Lett. **46**, 269 (1981).

[4]D. L. Neiman and B. E. Koel, in *Surface Chemistry of Thin Palladium Films,* in *Physical and Chemical Properties of Thin Metal Overlayers and Alloy Surfaces,* edited by D. M. Zehner and D. W. Goodman, MRS Symposia Proceedings No. 83 (Materials Research Society, Pittsburgh, 1988), pp. 143–153.

[5]M. W. Ruckman, P. D. Johnson, and M. Strongin, Phys. Rev. B **31**, 3405 (1985).

[6]B. E. Koel, R. Smith, and P. Berlowitz, Surf. Sci. **231**, 325 (1990).

[7]W. Schlenk and E. Bauer, Surf. Sci. **93**, 9 (1980).

[8]M. Tikhov and E. Bauer, Surf. Sci. **232**, 73 (1990).

[9]B. C. Bolding and E. A. Carter, Phys. Rev. B **42**, 11 380 (1990).

[10]D. Prigge, W. Schlenk, and E. Bauer, Surf. Sci. **123**, L698 (1982).

[11]M. Strongin, M. El-Batanouny, and M. Pick, Phys. Rev. B **22**, 3126 (1980).

[12]J. Heitzinger and B. E. Koel (private communication).
[13]M. W. Ruckman, V. Murgai, and M. Strongin, Phys. Rev. B **34**, 6759 (1986).
[14]M. Sagurton, M. Strongin, F. Jona, and J. Colbert, Phys. Rev. B **28**, 4075 (1983).
[15]R. Ramirez, A. Rahman, and I. K. Schuller, Phys. Rev. B **30**, 6208 (1984).
[16]J. H. van der Merwe and M. W. H. Braun, Appl. Surf. Sci. **22/23**, 545 (1985).
[17]E. Bauer and J. H. van der Merwe, Phys. Rev. B **33**, 3657 (1986).
[18]A. Kobayashi and S. Das Sarma, Phys. Rev. B **35**, 8042 (1987).
[19]S. M. Paik and I. K. Schuller, Phys. Rev. Lett. **64**, 1923 (1990).
[20]K. M. Knowles and D. A. Smith, Acta. Crystallogr. Sec. A **38**, 34 (1982).
[21]J. P. McTague and A. D. Novaco, Phys. Rev. B **19**, 5299 (1979).
[22]S. M. Foiles, M. I. Baskes, and M. S. Daw, Phys. Rev. B **33**, 7983 (1986).
[23]B. W. Dodson, Surf. Sci. **184**, 1 (1987).
[24]D. Wolf, Surf. Sci. **225**, 117 (1990).
[25]J. M. Eridon and S. Rao, *Derivation of Many-Body Potentials for Examining Defect Behavior in bcc Nb,* in Atomic Scale Calculations in Materials Science, edited by J. Tersoff, D. Vanderbilt, and V. Vitek, MRS Symposia Proceedings No. 141 (Materials Research Society, Pittsburgh, 1989), pp. 285–290.
[26]J. M. Eridon and S. Rao, Philos. Mag. Lett. **59**, 31 (1989).
[27]M. I. Haftel, T. D. Andreadis, J.V. Lill, and J. M. Eridon, Phys. Rev. B **42**, 11 540 (1990).
[28]J. B. Adams and S. M. Foiles, Phys. Rev. B **41**, 3316 (1990).
[29]The molecular-dynamics simulations were performed using the velocity form of the verlet algorithm with a time step of 1 fs.
[30]B. C. Bolding and E. A. Carter (unpublished).
[31]H. C. Anderson, J. Chem. Phys. **72**, 2384 (1980).